Investigating gene-environment interactions affecting methylmercury toxicity during embryonic development in zebrafish

Celia Dickey
Dr. Brad Carter

Abstract

Methylmercury (MeHg) is a common environmental contaminant in Wisconsin, and prenatal or early exposure to MeHg can cause developmental abnormalities. My research involves investigating gene-environment interactions of MeHg metabolism in embryonic development. MeHg is cleared from the body via oxidative stress metabolism pathways involving glutathione (GSH). The amount of time MeHg stays in the body varies across individuals. This diversity may be due to genetic polymorphisms in genes involved in MeHg metabolism. Certain alleles of GSH-related genes relate to elevated blood MeHg levels in adult humans; how these alleles affect MeHg metabolism in development is not well understood. This project aims to produce and validate mutant zebrafish lines with homozygous loss-of-function mutations in the *gclm* gene, a GSH-related gene associated with MeHg metabolism, using CRISPR-Cas9 reagents and high-resolution melt analysis genotyping (HRMA). The methods for this project were confirmed using CRISPR reagents targeting tyrosinase (*tyr*), a gene involved in pigment production. These results enable future experiments to characterize genetic influence on MeHg toxicity during development.

Introduction

Methylmercury; toxicology and metabolism

Methylmercury (MeHg) forms when bacteria react with inorganic mercury from industrial byproducts, water, air, soil, and plants. Bioaccumulation of MeHg can occur in aquatic food chains; small concentrations in small aquatic organisms accumulate to higher concentrations as the small organisms are eaten by larger fish. Once these fish are consumed, ingestion of the MeHg that has been accumulating throughout the food chain is released into the human body (Harding G, 2018). Once MeHg is in the body, it produces disulfides with a high chemical affinity to sulfhydryl groups from proteins. These disulfides are important for making protein structures and enzyme functions nonspecific as well as oxidative stress.

Atmospheric mercury comes from the burning of fossil fuels, mining, soil erosion, volcanic ash, and other environmental factors (Harding G, 2018) (Figure 1). Bacteria react with inorganic mercury in the water to form MeHg. When bacteria are digested by small organisms like phytoplankton, MeHg begins to accumulate in the food chain. As subsequent organisms digest smaller ones, the bioaccumulation of MeHg increases, leading to higher levels of MeHg in

aquatic organisms consumed by humans.

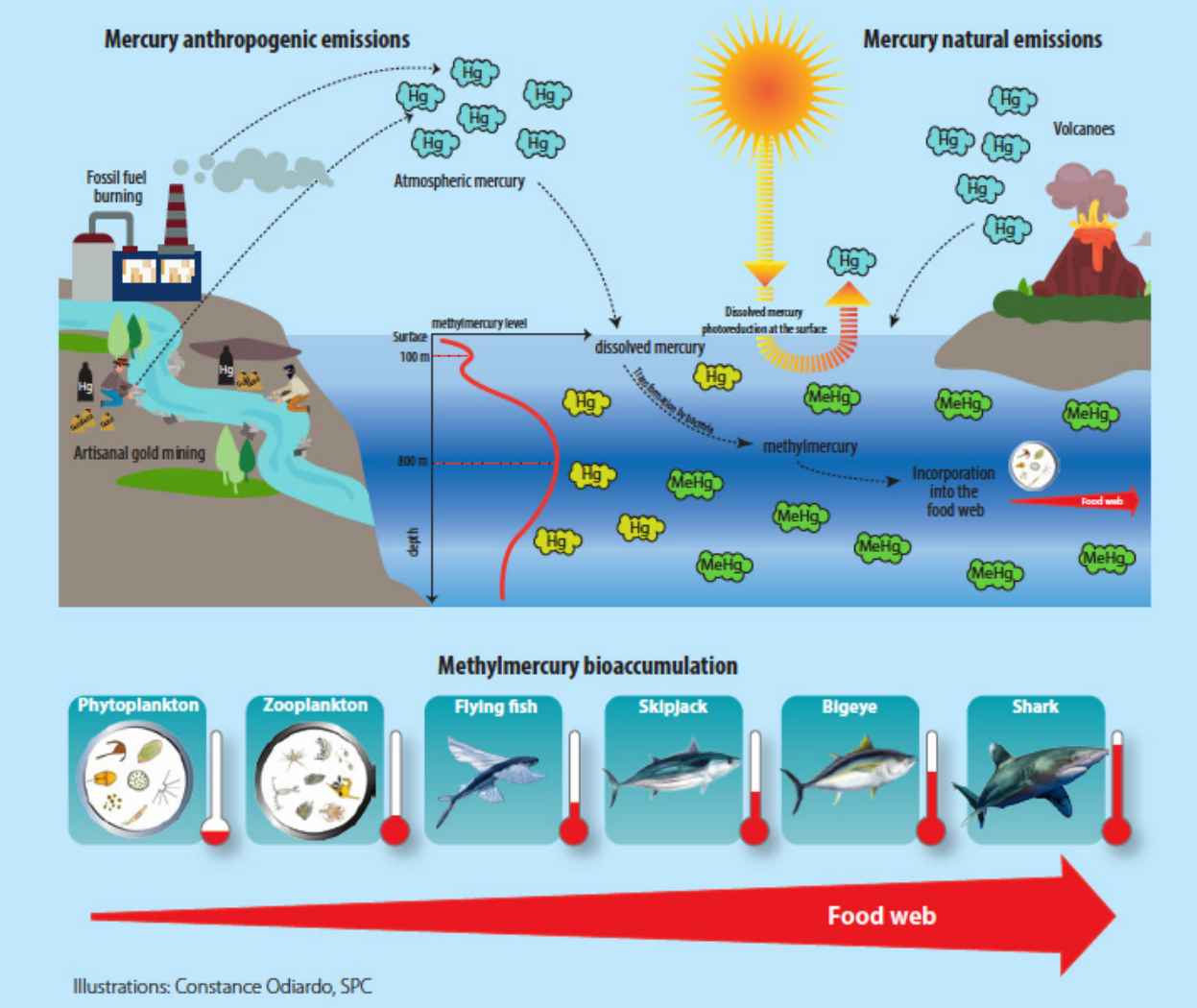

Figure 1. Sources of MeHg environmental contamination and bioaccumulation in food webs

MeHg is a common environmental pollutant in the Great Lakes area and is a known toxin to prenatal health and development. The upper level of MeHg considered to be safe is 5.8 parts per billion (ppb) for newborns in a bloodspot taken at birth. In the Lake Superior region, 1% of umbilical cord blood spots have levels above 58 ppb and a maximum of 211 ppb (McCann, 2011). Prenatally exposed children can display a wide range of effects from subtle developmental delays commonly associated with autism spectrum disorders to severe cerebral palsy (Castoldi et al., 2001). The effects of low-dose MeHg exposure are subtle and can include impaired motor function and sensory defects (Grandjean et al., 1999; Grandjean et al., 1997). In the nervous system, MeHg has been shown to inhibit protein synthesis, disrupt microtubule assembly, increase intracellular Ca2+, interfere with neurotransmitter function, and induce oxidative stress (Sanfeliu et al., 2003). Understanding the developmental effects of MeHg toxicity can inform

best prenatal health practices for pregnant mothers and their babies.

MeHg is removed from the body as a glutathione (GSH) conjugate. When MeHg enters a cell, it will bind to GSH, and the complex becomes a substrate for proteins that mediates cellular export of GSH conjugates out of the body (Ballatori, 2002). The amount of time MeHg remains in the body varies greatly across individuals from 30 to 150 days (Caito et al., 2018). This variation is due in part to genetic polymorphisms in the genes associated with the regulation of cellular MeHg. While the effects of prenatal MeHg exposure are well characterized after birth, this project aims to focus on the effects of MeHg exposure during prenatal development. These results will allow us to further understand gene-environment interactions of MeHg during prenatal development.

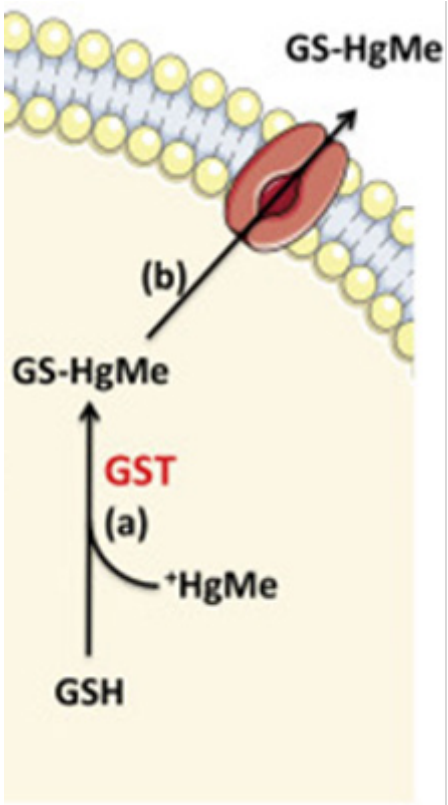

Figure 2. Pathway involved in the transportation of MeHg out of a cell encoded by the *gclm* gene. MeHg (depicted as HgMe) binds to a GSH conjugate to create a GS-MeHg complex (depicted as GS-HgMe) and is then transported out of the cell through the use of a regulatory membrane transport protein. *GCLM* is involved in production of GSH. Adapted from (Farina and Aschner, 2019).

GCLM is a gene that encodes a glutamate-cysteine ligase regulatory subunit involved in the synthesis of glutathione (GSH) from L-cysteine and L-glutamate. To remove MeHg from a cell, MeHg is attached by an enzyme to GSH and then transported as a GS-MeHg complex out of the cell (Carvan et al., 2004) (Figure 2). *GCLM* is involved in regulating GSH production and thus

regulating the cellular capacity to remove MeHg from the cell. Variants in the *GCLM* gene are found in the human population, leading to differences in the amount of time MeHg remains in the body.

Zebrafish as a Model Organism

We use zebrafish as our model organism due to its wide range of technical advantages in research. Zebrafish have a similar brain development and similar genomic DNA to humans. Zebrafish can be used for gene editing with CRISPR reagents (Carvan et al., 2004), an important feature for testing gene-environment interactions. Zebrafish have a transparent developmental stage that allows for characterization of visual mutations and aids in the process of fin-clipping for DNA isolation. Zebrafish also have a rapid early development and develop into mature adults 3 months post fertilization. Zebrafish yield a large number of embryos, enabling large sample sizes for experiments (Carvan et al., 2004). They are commonly used in biological research due to their small size, being easy to work with, and relatively inexpensive organisms. Of note for these experiments, zebrafish have a single homolog of *GCLM (gclm)*.

Zebrafish also have characterized genetic mutations that produce visible phenotypes. For example, tyrosinase (*tyr*) is a gene involved in the pigment production pathway (Figure 3). Blocking the function of this gene inhibits the pathway to produce melanin pigment, which results in little to no pigment production. Mutation in this gene is characterized as a visible phenotype (i.e. unpigmented embryos) that is used to confirm our microinjection techniques and reagents before targeting the *gclm* gene, which likely results in a non-visible phenotype. Brightfield microscopy can be used to visualize the loss of pigment production as a result of *tyr* mutation from Cas9-gRNA microinjection.

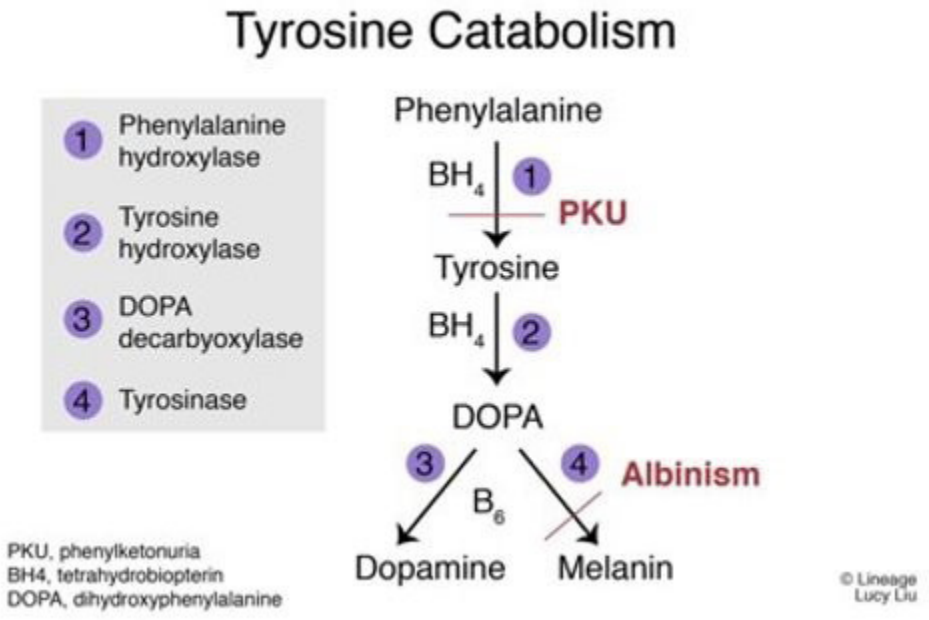

Figure 3. Pathway involved in the production of melanin. At step (4) in the pathway, tyrosinase acts to produce melanin. Blocking tyrosinase function results in albinism or an absence of melanin. Adapted from (Liu et al., 2021).

Methods

Breeding and Embryo Collection

Zebrafish of the EK strain were used for these experiments. Adult males and females are set up in breeding tanks the night before anticipated embryo collection to allow the zebrafish to acclimate in the tanks. A divider is inserted into the breeding tank to ensure timed breeding occurs. Timed breeding is important for this project to ensure that reagents are being injected into the single-celled embryonic stage. The divider is removed in the morning after the transition from the dark to light cycle. This transition is crucial for breeding since zebrafish breed shortly after the transition to the light cycle. Embryos are collected 10 minutes after the divider is removed. The embryos are rinsed to remove any debris and then placed into a petri dish with E3 solution prior to microinjection.

CRISPR/Cas9

CRISPR/Cas9 technology was developed from endonucleases found in bacterial and archaeal genomes. This technology involves sequence-guided DNA cutting by the Cas9 enzyme (Li et al., 2016). CHOPCHOP web tool was used to design a gRNA sequence to match the target DNA sequence in the gene of interest (Labun, 2019). gRNA was synthesized using a NEB EnGen kit (BioLabs). Using the synthesized gRNA with CRISPR/Cas9 reagents results in a mutation (insertion or deletion) that can lead to a loss-of-function within the gene (e.g. frameshift leading to premature stop codon).

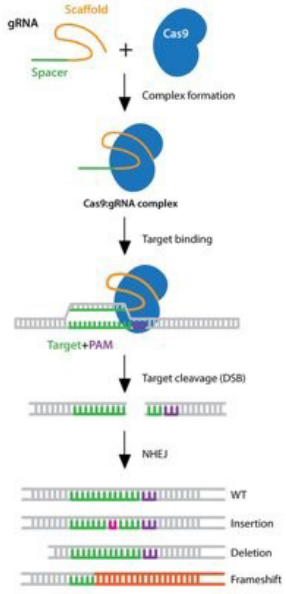

Figure 4. Diagram of CRISPR/Cas9 gene editing. Cas9 protein binds with the scaffold on targeted gRNA, forming a Cas9/gRNA complex. The spacer in the complex then binds to the target sequence adjacent to PAM sequence. Here, a double-stranded break is created, and the target sequence is cleaved resulting in an insertion, deletion, or frameshift mutation. Adapted from CRISPR Guide at Addgene (https://www.addgene.org/guides/crispr/#web-references).

Microinjection

The microinjection process involves combining CRISPR/Cas9 protein with gRNA, designed to match our target DNA sequence, nuclease-free water, and phenol red dye. Phenol red dye enables visualization of the injection of reagents into the embryo. Once the reagents are combined, the contents are pipetted into a capillary needle and inserted into the microinjection apparatus. When the needle was secure, a specialized slide was placed on the microscope and a drop of mineral oil was added to the center of the circle. The needle was cut using forceps to obtain a diameter of injected reagents of 1nL. Embryos were added to the agarose well-plate with E3 solution and were injected with the CRISPR/Cas9 and gRNA reagents. After the injection of CRISPR/Cas9 and gRNA reagents, embryos were transferred into a new petri dish with E3 solution. After completion of all injections, petri dishes were placed into an incubator set at ~28.5 degrees Celsius.

Fin Clipping

At 3 days post fertilization (dpf), zebrafish that were injected with *gclm* gRNA and CRISPR/Cas9 reagents undergo fin-clipping. 3-4 zebrafish were placed into a petri dish filled with E3 and 2-4 drops of tricaine solution to anaesthetize them. Once the zebrafish were anaesthetized, a single fish is placed onto a petri dish lid covered with scotch tape and arranged under the microscope. A scalpel was used to cut the end of the tail off between the end of the tail and the return artery of blood flow. Forceps were used to collect the tail sample and placed into the corresponding PCR tube with NaOH and labeled with the fish number. Once finished, the scalpel and forceps were sterilized with ethanol and wiped dry with a Kimwipe. A short period of observation is necessary to make sure the artery was not cut, and the fish will not die from a loss of blood. The fish were collected and placed into a recovery dish filled with E3 solution. Once recovered, the fish were placed back into their corresponding well in the multi-well plate with E3 solution and placed into an incubator set at ~28.5 degrees Celsius (Wilkinson et al., 2013). The clipped fins are now ready for DNA isolation. PCR tubes were heated at 95 degrees Celsius for 10 minutes with a cool-down period at 4 degrees Celsius for 30 seconds in the thermocycler. 2 uL of 1M Tris pH 8.0 was added to each PCR tube to neutralize NaOH, then spun down in a centrifuge. The supernatant containing the DNA was pipetted off, placed into new PCR tubes, and stored at -20 degrees Celsius (Meeker et al., 2007).

High Resolution Melt Analysis

High Resolution Melt Analysis (HRMA) genotyping is a quantitative analysis of a melt curve after polymerase chain reaction (PCR) amplification. HRMA measures small changes in DNA sequence by measuring the fluorescence signals in each sample and is reported to detect as small as a single base change in a DNA sequence (Wilkinson et al., 2013). These changes in fluorescence indicate a genetic difference between the samples, measured in Relative Fluorescence Units (RFU). PCR primers for the genes of interest are designed using the CHOPCHOP web tool (Labun, 2019). Synthetic DNA templates were used to model variations in HRMA signals of different PCR product lengths. PCR templates containing 5bp deletion and10bp deletion model the expected difference in RFU signal due to a mutation of these lengths at the target site. The full-length template models the signal of the sequence with no mutation, matching wild-type/reference RFU signal. Synthetic templates were ordered as DNA oligonucleotides from IDT.

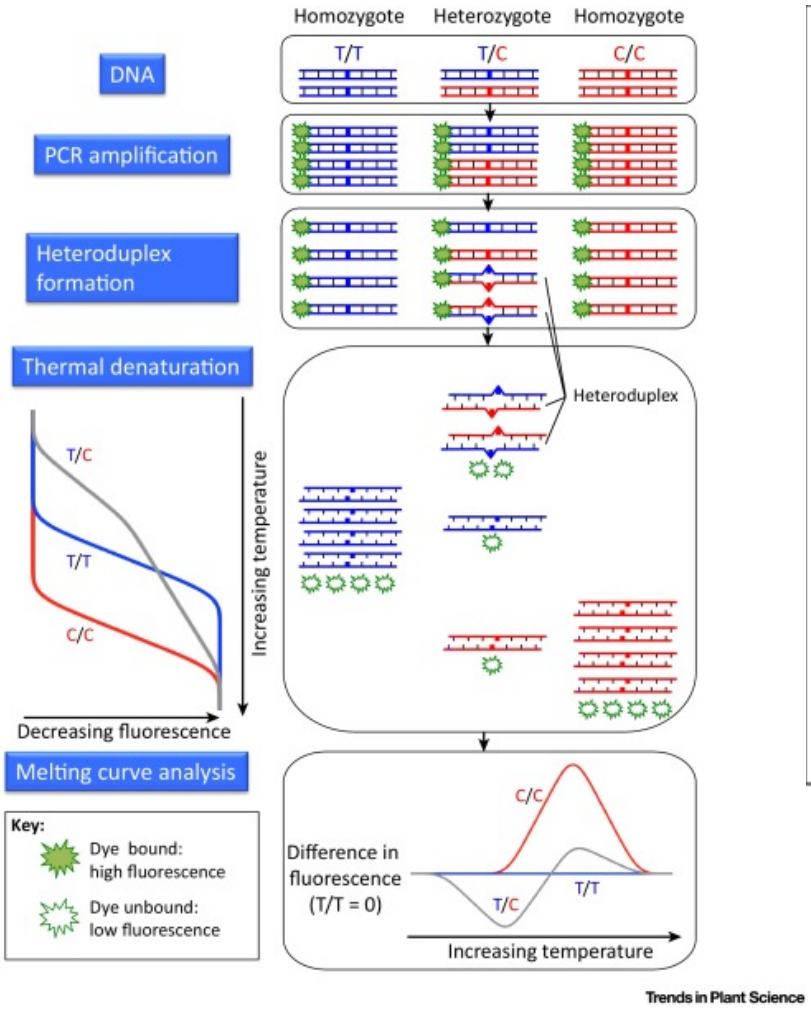

Figure 5. Diagram of HRMA procedure. PCR amplification makes copies of the DNA sequence. Then, the fluorescence dye is bound to the DNA and undergoes thermal denaturation, separating the two DNA strands. The fluorescence signals are measured against a specified reference sample to get the Difference RFU value. Differences in DNA sequence result in different denaturation kinetics, producing distinct patterns of fluorescence signal by genotype. Adapted from (Simko et al., 2016).

Results

CRISPR and HRMA genotyping were used to create knockout zebrafish lines. *tyr* mutants have a distinguishable difference in pigment production, most visible within the eye cells, making them more transparent and allowing individual eye cells to be more distinguishable (Figure 6). Reduced pigment production can also be seen along the spine and on the yolk. The results shown in figure 6 indicate mutation of the target gene, validating the microinjection technique and our process of developing CRISPR/Cas9 reagents.

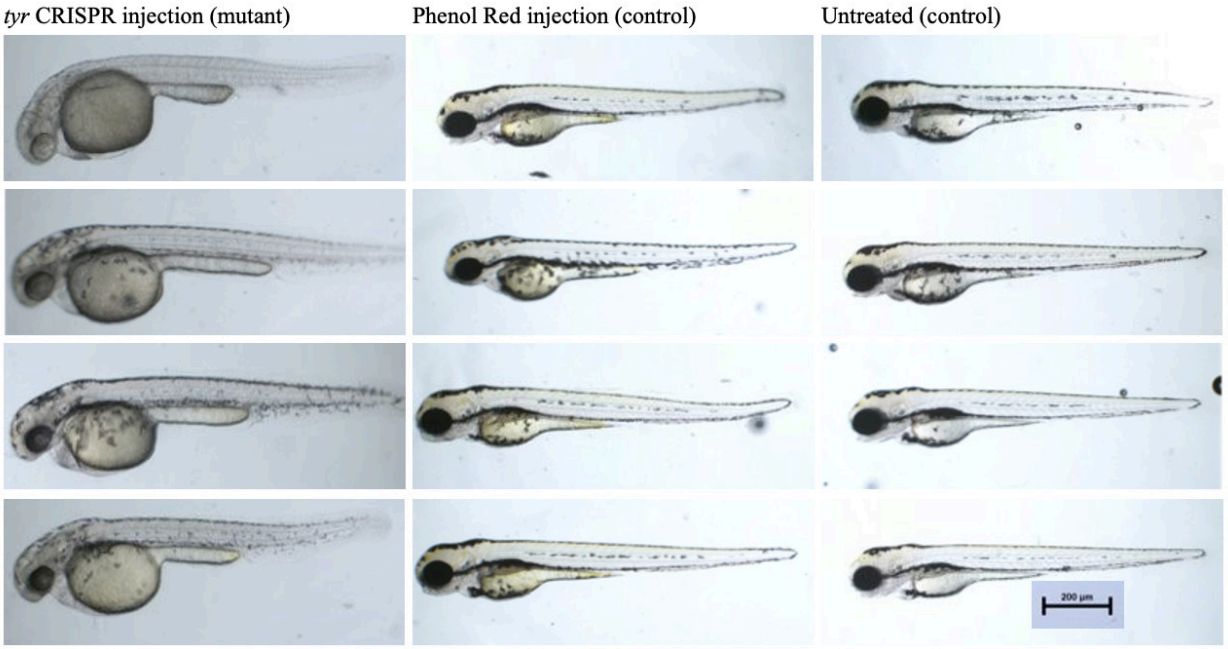

Figure 6. Zebrafish injected with *tyr* CRISPR reagents show pigmentation changes, indicating genetic mutation. The left column of zebrafish shows the *tyr* mutant phenotype; the middle column shows the phenol red phenotype (injection control); and the right column is wild-type (clutch control). The difference in pigment production is most distinguishable within eye cells. Images were taken with a Nikon SMZ1500 (C-DSD115) scope at at 3 dpf.

Using HRMA genotyping, we were able to confirm *tyr* mutations from our CRISPR reagents. The *tyr* DNA sequences modeling 5bp deletion and 10bp deletion produced RFU differences of 0.06 compared with full-length wild-type DNA sequence (Figure 7). We thus predicted a similar CRISPR-induced mutation would have a similar difference in RFU. The HRMA genotyping experiment with *tyr* injected fish DNA observed a Difference RFU value of 0.065 (figure 8), suggesting a similar change in sequence to these altered DNA sequences.

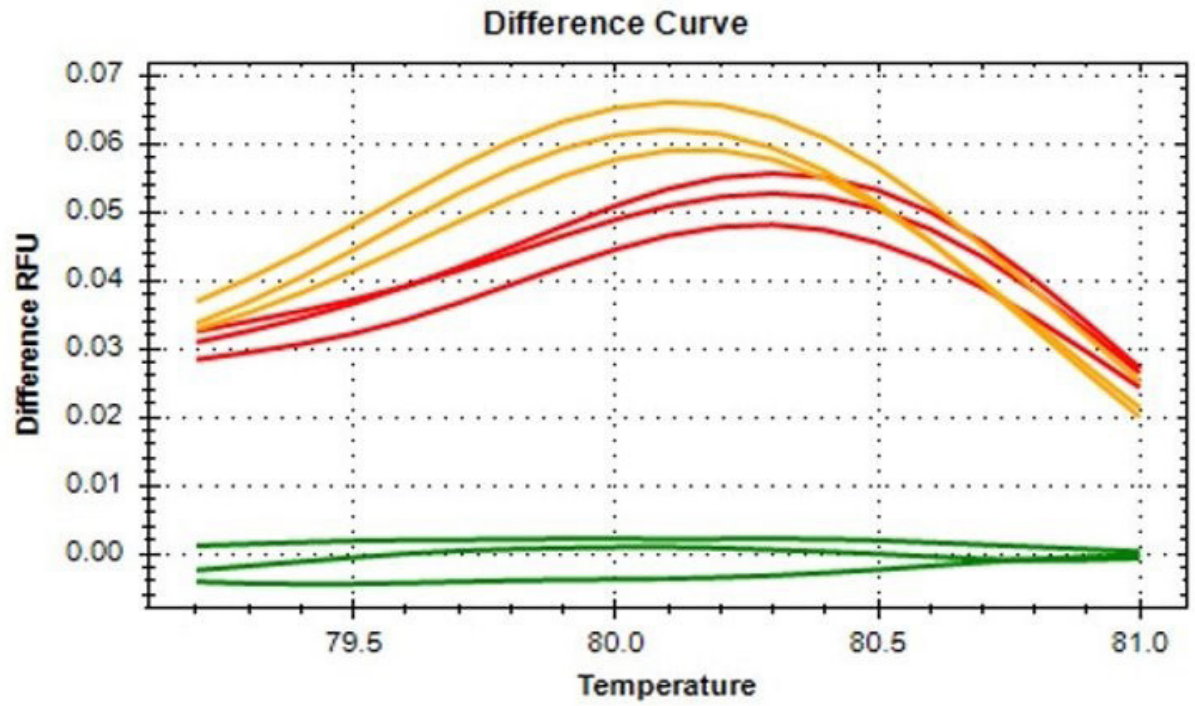

Figure 7. HRMA genotyping distinguishes between DNA templates for *tyr*. Primers for *tyr* were used with synthetic DNA templates with differing base pair lengths to model CRISPR-induced deletions (WT vs 5bp deletion vs 10bp deletion). Results show an expected Difference RFU value of 0.06 for CRISPR-induced deletions. (WT-green, 5bp deletion- yellow, 10bp deletion-red). Each line represents an individual HRMA reaction (technical triplicates). Values were referenced to the WT template.

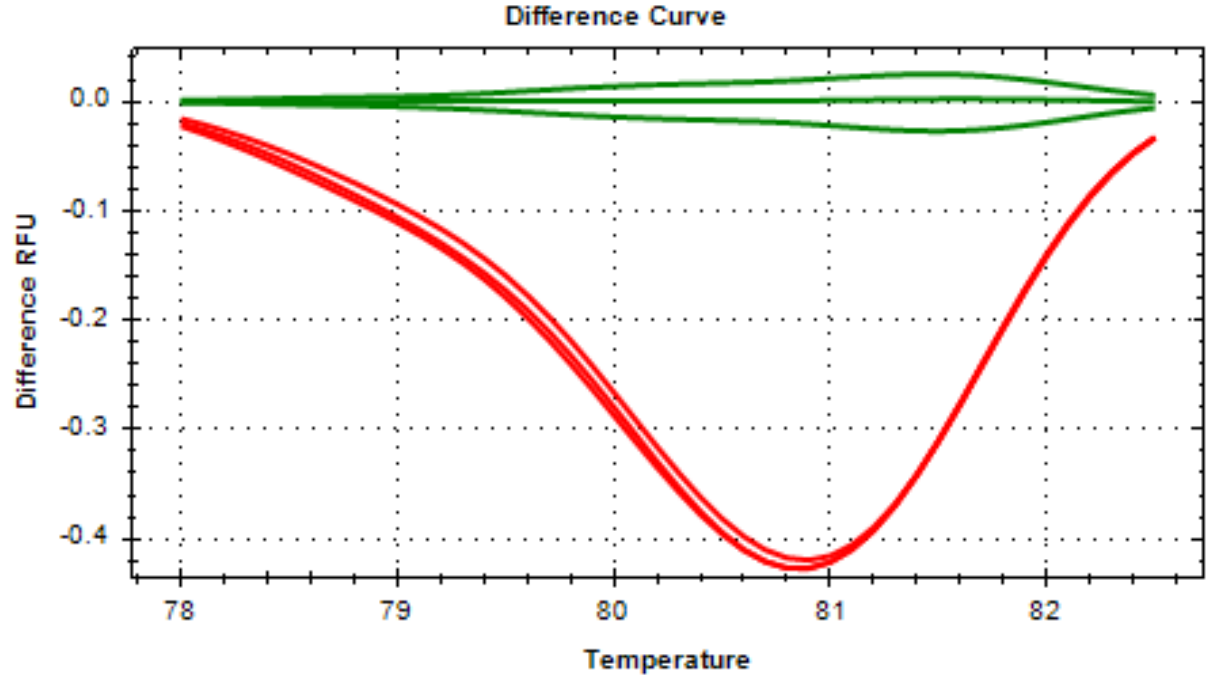

Figure 8. HRMA genotyping distinguishes between *tyr* mutants and WT fish. A portion of *tyr* mutants (red, n=24) had apparent distinguishable Difference RFU compared to WT (green, n=7) and phenol red control (blue, n=8). WT and phenol red control do not have a distinguishable Difference RFU. Each line represents DNA from an individual fish. Values were referenced to the WT control group.

Using HRMA genotyping, we were able to confirm *gclm* mutations from CRISPR reagents. The *glcm* DNA sequences modeling 10bp deletions produced RFU differences of 0.4 compared with full-length wild-type DNA sequence (Figure 9). We thus predicted a similar CRISPR-induced mutation would have a similar difference in RFU. The HRMA genotyping experiment with *gclm* injected fish DNA observed a Difference RFU value of 0.45 (figure 10A and 10B), suggesting a similar change in sequence to these altered DNA sequences.

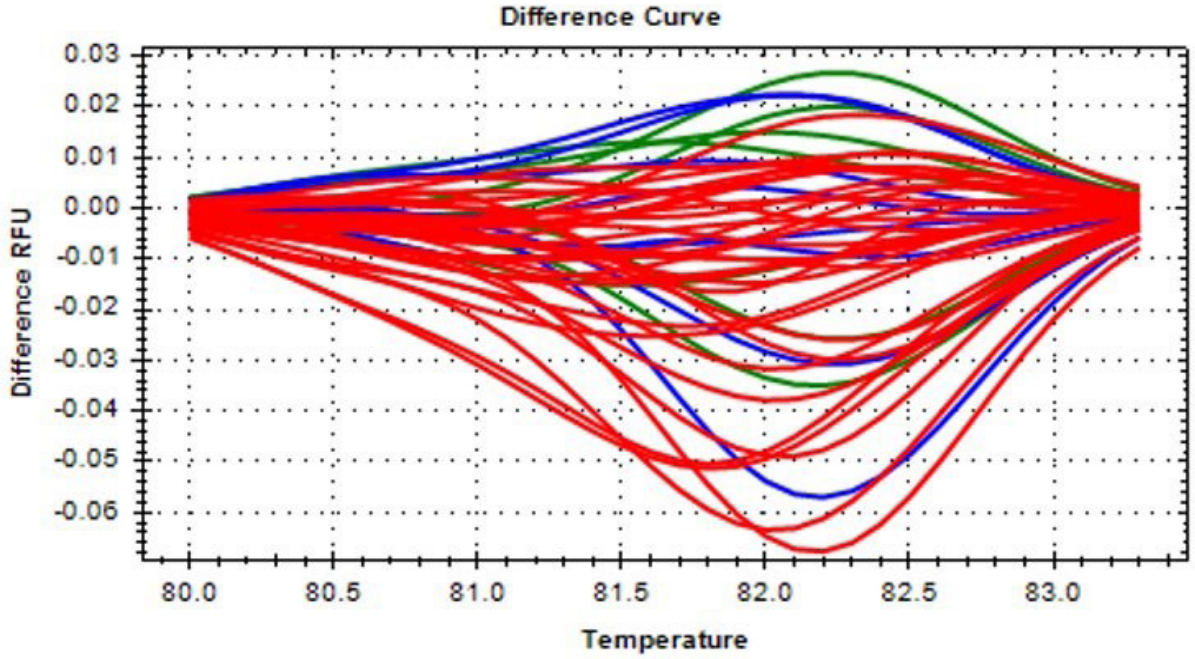

Figure 9. HRMA genotyping distinguishes between DNA templates for *GCLM*. Primers for *GCLM* were used with synthetic DNA templates to model CRISPR-induced deletions; WT (green), 10bp deletion (red). Results show an expected Difference RFU value of 0.4 for CRISPR-induced deletions. Each line represents an individual HRMA reaction (technical triplicates). Values were referenced to the WT template.

The first HRMA genotyping experiment with *GCLM* injected fish DNA observed a Difference RFU value of 0.4 (figure 10A), suggesting mutation similar to the 10bp template. The second HRMA genotyping experiment with *GCLM* injected fish DNA observed a Difference RFU value of 0.5 (figure 10B), suggesting a larger change in the sequence than initially suspected.

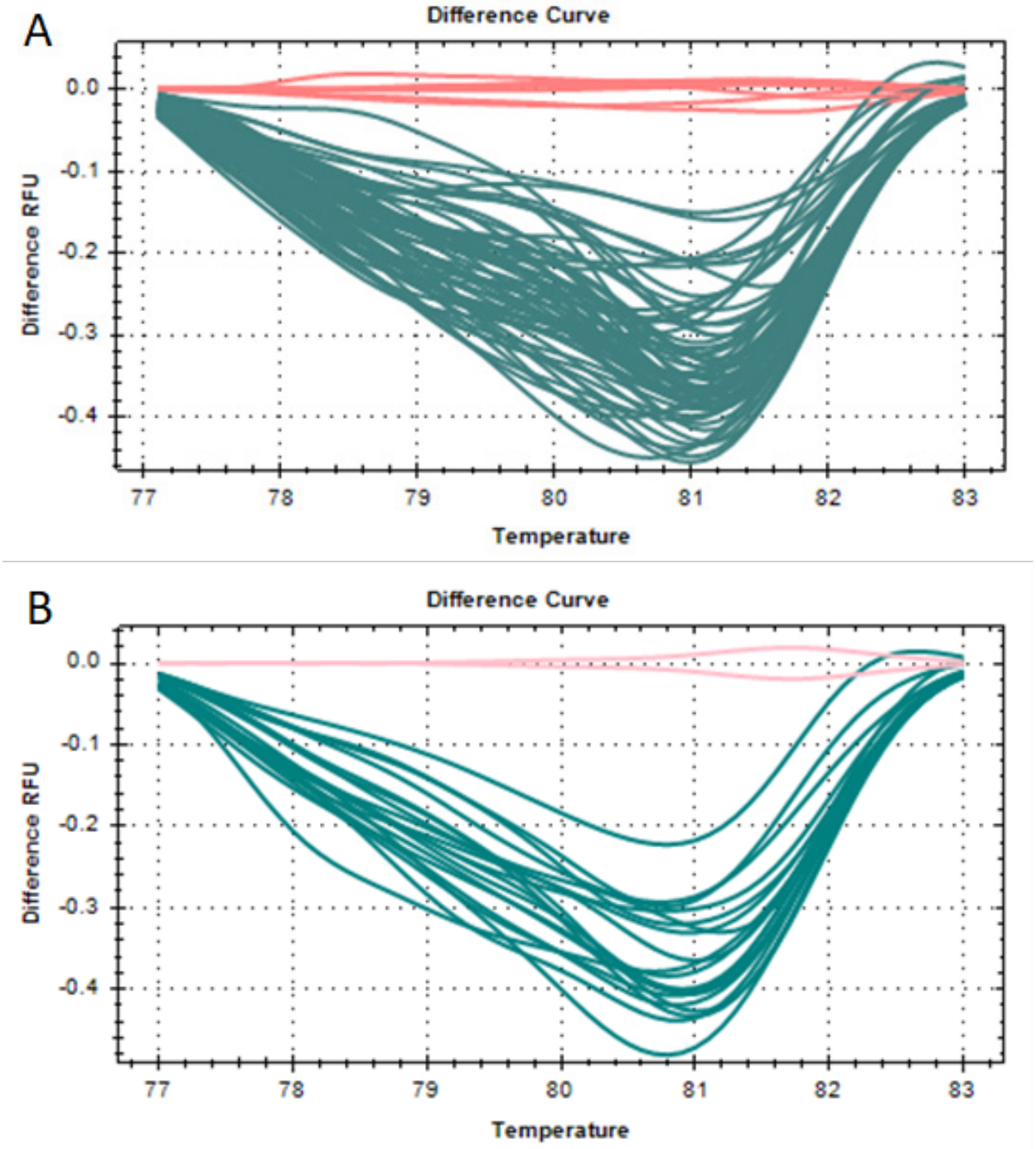

Figure 10. HRMA genotyping distinguishes between *gclm* mutants and WT fish. (a) A majority of *gclm* mutants (teal, n=62) had apparent distinguishable Difference RFU compared to WT (pink, n=8) with a value of 0.45. Values were referenced to the WT control group. **(b)** A portion of *gclm* mutants (teal, n=19) had apparent distinguishable Difference RFU compared to WT (pink, n=2) with a value of 0.45. Values were referenced to the WT control group.

Overall, the mutant samples are consistently different than the wild-type samples in both experiments, allowing us to be confident there is a mutation occurring. Validating these results

and identifying associated DNA sequence changes is the next step in creating a *gclm* knockout zebrafish line.

Discussion

The effects of MeHg exposure have been characterized after birth but are not well understood during human development. The overall goal of this project is to better understand neurological development in response to MeHg toxicity. We have been able to successfully create *gclm* mutations in zebrafish. We have raised the P0 generation that likely contain mutations of the *gclm* gene and are currently working toward characterizing mutation DNA sequences to identify loss-of-function alleles.

Future Directions

We intend to raise a transgenic mutant zebrafish line to test MeHg toxicity on homologous loss-of-function embryos and compare results to WT zebrafish. The next steps for this project are to create and validate a *GCLM* mutant zebrafish line by confirming the inherited mutation and determining the sequence of the mutation to ensure a loss-of-function allele. Outcrossing with WT zebrafish will be done to make F1 heterozygotes. The F1 generation will be raised and in-crossed to produce F2 homozygotes. After producing a transgenic mutant zebrafish line, we plan to test the effects of MeHg on social, motor, visual, and learning development of zebrafish compared to WT zebrafish.

A long-term future direction includes using human variants in *GCLM* on MeHg toxicity by combining our *gclm* knockout zebrafish with lines expressing human *GCLM* variants (collaboration with Carvan lab at UW-Milwaukee). Additionally, CRISPR/Cas 9 reagents and HRMA genotyping will be used to knock out additional genes related to GSH-production (gstp1, gstp2, gclc). This project will create a stronger understanding of the relationship between MeHg exposure and neurodevelopmental deficits.

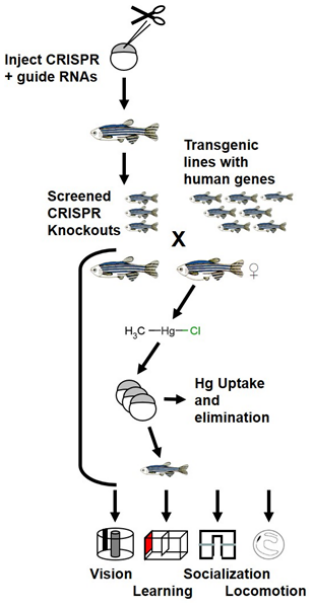

Figure 11. Schematic of current and future project experiments.

References

Ballatori, N. (2002). Transport of toxic metals by molecular mimicry. Environ Health Perspect *110 Suppl 5*, 689-694. 10.1289/ehp.02110s5689.

BioLabs EnGen® sgRNA Synthesis Kit, *S. pyogenes* Protocol (NEB #E3322). BioLabs.

Caito, S.W., Jackson, B.P., Punshon, T., Scrimale, T., Grier, A., Gill, S.R., Love, T.M., Watson, G.E., van Wijngaarden, E., and Rand, M.D. (2018). Editor's Highlight: Variation in Methylmercury Metabolism and Elimination Status in Humans Following Fish Consumption. Toxicol Sci *161*, 443-453. 10.1093/toxsci/kfx226.

Carvan, M.J., 3rd, Loucks, E., Weber, D.N., and Williams, F.E. (2004). Ethanol effects on the developing zebrafish: neurobehavior and skeletal morphogenesis. Neurotoxicol Teratol *26*, 757-768. 10.1016/j.ntt.2004.06.016.

Castoldi, A.F., Coccini, T., Ceccatelli, S., and Manzo, L. (2001). Neurotoxicity and molecular effects of methylmercury. Brain Res Bull *55*, 197-203. 10.1016/s0361-9230(01)00458-0.

Grandjean, P., Budtz-Jørgensen, E., White, R.F., Jørgensen, P.J., Weihe, P., Debes, F., and Keiding, N. (1999). Methylmercury exposure biomarkers as indicators of neurotoxicity in children aged 7 years. Am J Epidemiol *150*, 301-305. 10.1093/oxfordjournals.aje.a010002.

Grandjean, P., Weihe, P., White, R.F., Debes, F., Araki, S., Yokoyama, K., Murata, K., Sørensen, N., Dahl, R., and Jørgensen, P.J. (1997). Cognitive deficit in 7-year-old children with prenatal exposure to methylmercury. Neurotoxicol Teratol *19*, 417-428. 10.1016/s0892-0362(97)00097-4.

Harding G, D.J., Vass P (2018). Bioaccumulation of methylmercury within the marine food web of the outer Bay of Fundy, Gulf of Maine. PLoS ONE *13*. https://doi.org/10.1371/journal.pone.0197220.

Labun, K., Montague, T. G., Krause, M., Torres Cleuren, Y. N., Tjeldnes, H., & Valen, E. (2019). CHOPCHOP v3: expanding the CRISPR web toolbox beyond genome editing. Nucleic Acids Research.

Li, M., Zhao, L., Page-McCaw, P.S., and Chen, W. (2016). Zebrafish Genome Engineering Using the CRISPR-Cas9 System. Trends Genet *32*, 815-827. 10.1016/j.tig.2016.10.005.

McCann, P. (2011). Mercury Levels in Blood from Newborns in the Lake Superior Basin.

Meeker, N.D., Hutchinson, S.A., Ho, L., and Trede, N.S. (2007). Method for isolation of PCR-ready genomic DNA from zebrafish tissues. Biotechniques *43*, 610, 612, 614. 10.2144/000112619.

Sanfeliu, C., Sebastià, J., Cristòfol, R., and Rodríguez-Farré, E. (2003). Neurotoxicity of organomercurial compounds. Neurotox Res *5*, 283-305. 10.1007/bf03033386.

Wilkinson, R.N., Elworthy, S., Ingham, P.W., and van Eeden, F.J. (2013). A method for high-throughput PCR-based genotyping of larval zebrafish tail biopsies. Biotechniques *55*, 314-316. 10.2144/000114116.